IEEE Access
Multidisciplinary | Rapid Review | Open Access Journal

Received August 28, 2019, accepted September 13, 2019, date of publication September 19, 2019, date of current version October 2, 2019.

Digital Object Identifier 10.1109/ACCESS.2019.2942350

An Efficient Hybrid Beamforming Design for Massive MIMO Receive Systems via SINR Maximization Based on an Improved Bat Algorithm

MOHAMMED A. ALMAGBOUL[1,2,3], FENG SHU[1,4,5], YAOLU QIN[1], XIAOBO ZHOU[1], JIN WANG[6], YUWEN QIAN[1], KINGSLEY JUN ZOU[1], AND ABDELDIME MOHAMED SALIH ABDELGADER[7]

[1]School of Electronic and Optical Engineering, Nanjing University of Science and Technology, Nanjing 210094, China
[2]Electronic Engineering Department, Algraif Sharg Technological College, Sudan Technological University, Khartoum 13315, Sudan
[3]Communication Engineering Department, AlMughtaribeen University, Khartoum 11123, Sudan
[4]College of Computer and Information Sciences, Fujian Agriculture and Forestry University, Fuzhou 350002, China
[5]College of Physics and Information, Fuzhou University, Fuzhou 350116, China
[6]Shanghai Aerospace Electronic Technology Institute, Shanghai 201109, China
[7]Electrical and Computer Department, College of Engineering, Karary University, Khartoum 12304, Sudan

Corresponding authors: Kingsley Jun Zou (jun_zou@njust.edu.cn) and Mohammed A. Almagboul (almagboul@njust.edu.cn)

This work was supported in part by National Natural Science Foundation of China under Grants 61901121, 61701234, and 61771244, and in part by the Natural Science Research Project of Education Department of Anhui Province of China under Grant KJ2019A1002.

ABSTRACT Hybrid analog and digital (HAD) beamforming has been recently receiving considerable deserved attention for practical implementation on the large-scale antenna systems. Compared to fully-digital beamforming, partially-connected HAD beamforming can significantly reduce the hardware cost, complexity, and power consumption. This paper aims to mitigate interference and increase robustness against direction-of-arrival (DOA) mismatch along with lowering hardware complexity, cost, and power dissipation. To achieve these goals, a novel robust HAD beamforming receiver with partially-connected structure is proposed. It is based on methods of an improved bat algorithm (I-BA) and robust adaptive beamformers (RABs) in the digital domain. Since most of the RAB methods are sensitive to the DOA mismatch and depending on the complex weights which lead to an expensive receiver, the I-BA is proposed. In the analog part, analog phase alignment by linear searching (APALS) with sufficiently fine grid points is employed to optimize the analog beamforming matrix. The performance of the proposed I-BA is assessed using MATLAB simulation and compared with BA, and particle swarm optimization (PSO) algorithms. It shows better performance in terms of convergence speed, stability, and convergence rate. Besides, the proposed hybrid I-BA-APALS approach showed better performance compared to other proposed robust hybrid techniques, i.e., diagonal loading (DL) APALS (DL-APALS) and DL spatial matched filter (SMF) APALS (DL-SMF-APALS).

INDEX TERMS Beamforming, MIMO wireless systems, SINR, wireless communications.

I. INTRODUCTION

Although the initial applications of adaptive beamforming were in military areas, its use in civilian applications has also gained great popularity today [1]. Adaptive beamforming has well-known advantages such as interference suppression and enhancing the system capacity. This is done by steering the antenna array's main beam pattern toward the desired signal, while steering the nulls toward the directions of interference signals. In a hybrid system, this can be accomplished by constantly updating the total beamforming weights. The widespread of wireless devices has led to the multiplicity and diversity of interference sources. Therefore, adaptive beamforming will be one of the most important techniques in wireless communication systems for interference suppression [2].

The immense hardware cost and power consumption of massive multiple-input-multiple-output (MIMO) systems are

The associate editor coordinating the review of this manuscript and approving it for publication was Shuai Han.

considered among the most design challenges. This is particularly so in the classical massive MIMO system, where each antenna is connected to one radio frequency (RF) chain. This results in a remarkably high hardware cost, complexity, and power consumption [3]. Consequently, the use of the hybrid analog and digital (HAD) beamforming received great interest from researchers, due to the promising practical implementation in the massive MIMO systems for the fifth-generation (5G) communications [4]. Compared to a fully-digital beamforming design, HAD beamforming requires fewer numbers of RF chains [5], [6]. Moreover, HAD beamforming combines the accuracy and speed features of digital beamforming and the inexpensive characteristic of analog beamforming [7], [8].

Nature-inspired optimization algorithms are widely used for adaptive beamforming to address the restrictions of conventional adaptive optimization algorithms. Algorithms based on error-derivative methods such as linearly constrained minimum variance (LCMV), and minimum variance distortionless response (MVDR) suffer from inflexibility and getting stuck in local minima. Besides, it needs accurate knowledge of directions of arrival (DOA) of interference signals [7], [9], [10]. Recently, the employment of metaheuristic algorithms in the array pattern synthesis has received great interest from researchers. This is due to its flexibility, and being able to deal with non-convex and nondifferentiable optimization problems [9]–[13]. Genetic algorithm (GA) [14] is one of the ancient and well-known nature-inspired techniques. It has been used early for synthesizing pattern of antenna arrays [15]. Particle swarm optimization (PSO) [16] is another widely known swarm-based algorithm; It is faster, efficient, easier to implement, and has a capability of solving linear and nonlinear optimization problems. PSO is used extensively in designing antenna arrays [17], [18]. A lot of other metaheuristic optimization algorithms have been also employed successfully in antenna array synthesizing [12], [19]–[21], such as the ant-lion optimization (ALO) technique introduced in [22], grey wolf optimizer (GWO) [23], cat swarm optimization (CSO) [24], ant colony optimization (ACO) [25], invasive weed optimization (IWO) [26], simulated annealing (SA) [27], whale Optimization algorithm (WOA) [28], and others.

The Bat Algorithm (BA) is a swarm intelligence algorithm initiated by Yang in 2010 [29]. It is inspired from the nature behavior of bats, which uses echolocation by changing pulse rates of emission and loudness to detect prey and avert obstacles. A number of researchers have used BA for linear antenna array (LAA) to steer nulls and minimize sidelobe level (SLL). Van Luyen and Giang [10] proved that the BA can outperform the accelerated particle swarm optimization (APSO) and GA in terms of adaptive null-steering, sidelobe suppression, and computation time in array pattern synthesis using phase-only control. In [30] again they utilize BA in order to minimize SLL and to place nulls in the desired directions using amplitude-only control. It has been proven that the BA based beamformer is more effective and faster as compared to GA and APSO. In [31] BA based beamformer using complex weight (amplitude and phase) compared with APSO shows faster convergence and higher efficiency. However, the above and a lot of other researches using different metaheuristic optimization algorithms mainly concentrate on the fully-digital beamforming instead of HAD beamforming. To best of our knowledge, very few employments of these algorithms in HAD beamforming were carried out [32]–[36].

In [34], [35] the authors proposed a phase-only HAD beamforming based on GA with the aim of minimizing the transmit power under signal-to-interference-plus-noise ratio (SINR) constraints. Based on the particle swarm ant colony optimization (PSACO) algorithm, in [36], a partially-connected hybrid precoding structure for wideband massive MIMO systems is proposed in order to realize excellent energy and spectral efficiency. In [33], based on a genetic algorithm (GA), a joint precoding in the multiuser MIMO (MU-MIMO) system with the objective of maximizing the capacity is carried out. The authors in [32] proposed two HAD beamformers based on PSO and manifold optimization (MO) for capacity maximization. However, all these research activities mostly focus on a transmitter not receiver. These proposed beamformers were mainly concentrating on such objective issues as rate maximization [37], [38], secrecy rate maximization [39], maximizing signal-to-leakage-and-noise ratio (Max-SLNR) per user [40], [41], and transmit/receive power minimization/maximization [3], while often neglecting the aspect of robustness. On the other hand, considerably less attention has been paid to the partially-connected structure [3], [38], [42], [43].

The authors in [3] proposed two low complexity phase alignment methods for average receive power maximization of partially-connected hybrid structure. The proposed methods for direction angles estimation are root multiple signal classification-hybrid digital and analog PA (Root-MUSIC-HDAPA) and HDAPA. However, these methods may result in a performance loss of interference reduction due to the DOAs' estimation errors. Further, the system model in [3] is designed to support only one desired signal and no interferences. Reference [38] proposed a semidefinite relaxation based alternating minimization (SDR-AltMin) algorithm for transmission rate optimization of the hybrid partially-connected structure. The work in [42], which considered a wideband uplink MIMO system, showed that the digital beamforming with low resolutions analog-to-digital converter (ADC) can achieve a higher rate and energy-efficient as compared to the partially-connected hybrid receiver. However, the tight space constraints in a full digital massive array remains a challenge. Assuming perfect knowledge of the channel state information (CSI), [43] introduced achievable rates of partial-connected hybrid precoding in MU-MIMO system when utilizing only one RF chain per user. For each user (receiver), the analog combiner is obtained using singular value decomposition (SVD) algorithm. Based on a low complexity Gram-Schmidt method, the work in [44]

is proposed for uplink multiuser fully-connected hybrid system. The main idea is to address the inter-user interference and to maximize the effective gain.

This paper focuses on an efficient interference suppression at the receiver for the partially-connected HAD beamforming structure. Our goal is to maximize the SINR in the case of the presence and absence of DOA mismatches. Some research activities provide improvements on the BA to avoid the weaknesses of the algorithm being trapped in the local minima or yielding unstable results [45]–[47]. The main distinctions between the Improved-BA (I-BA) and the BA are the bats' compensation for Doppler effects in echoes, and the possibility of selecting different habitats; this makes the algorithm further imitating the bats' behaviors and thus improves the stability and efficiency. The main contributions of this paper are summarized as follows:

1) Presents an I-BA and analyzes its special properties and excellent features in terms of adaptive beamforming. I-BA allows us to optimize the digital beamformer's weights using the phase-only, so that a receiver design will have less hardware cost and complexity.
2) Formulating the objective functions for the SINR maximization based hybrid beamforming optimization model under the partially-connected HAD receiver. Besides, two simple hybrid algorithms are proposed for single and multiple data streams.
3) By means of a closed-form solution of digital beamforming vector, combinations of analog phase alignment by linear searching APALS) in the analog part and diagonal loading (DL) methods [48] in the digital domain are proposed. For better performance, a spatial matched filter (SMF) method is adopted, which is a good way of choosing the loading level [49]. Simulation results show that the proposed I-BA-APALS-based hybrid beamforming method outperforms DL-based hybrid methods, i.e., DL-APALS and DL-SMF-APALS in terms of nulls depth, robustness, and the SINR maximization.

The rest of this work is structured as follows: our system model of partially-connected HAD beamforming is defined. In section III, the problem is formulated. Thereafter, the proposed Improved-BA is described, and the results are discussed in Section IV and V, respectively. Finally, the conclusions are given in Section VI.

Notation: Capital X, boldface small $\mathbf{x}$, and small x letters are used to represent matrices, vectors, and scalars, respectively. Notations $(\cdot)^T$ and $(\cdot)^H$ denote transpose and conjugate transpose of a matrix, respectively. $|\,x\,|$ denotes the magnitude of a complex number x and the norm is denoted by $\|x\|$. $\mathbb{E}\{\cdot\}$ denotes the expectation operation.

II. SYSTEM MODEL

Consider a partially-connected HAD beamforming structure at the receiver, as shown in Fig. 1. This structure is used to reduce hardware cost and energy consumption with somewhat less performance. The receiver is chosen to be equipped

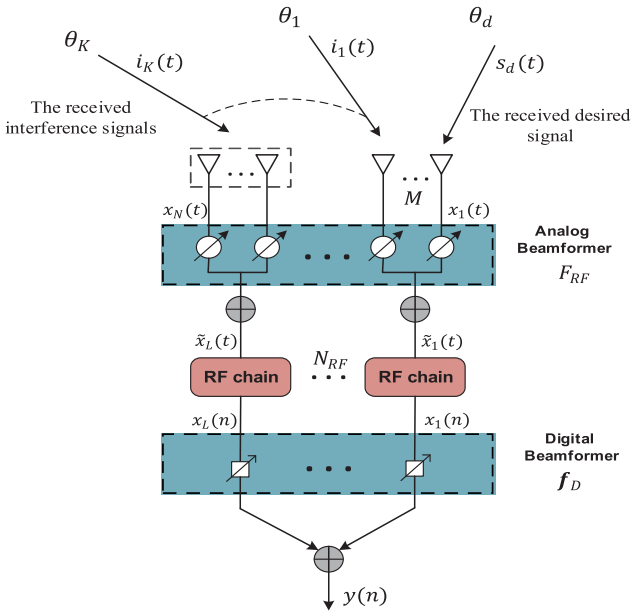

FIGURE 1. Partially-connected HAD beamforming structure at the receiver.

with N isotropic antennas divided into L subsets of antenna arrays, and each subset contains M antenna elements. The number of RF chains N_{RF} is chosen to be less than the number of antenna elements $N_{RF} \leq N$. Each subset of antenna array elements is connected to only one RF chain. The antenna elements are followed by phase shifters that feed the RF chains. The hybrid beamforming of Fig.1 receives one desired signal $s_d(t)\,e^{j2\pi f_c t}$ with an angle of arrival (AOA) θ_d, and K interference signals $i_k(t)\,e^{j2\pi f_c t}$ with different angles of arrival θ_k, $k = 1, \ldots, K$. The received signals $x_m(t)$ of the l-th sub-array at the input of each m-th element ($m = 1, \ldots, M$) include the desired narrow band signal, the interference narrow band signals, and an additive white Gaussian noise (AWGN) $v(t)$ with zero mean and variance σ_v^2. Therefore, the l-th sub-array output $\tilde{x}_l(t)$ can be represented as follows

$$\begin{aligned}\tilde{x}_l(t) = &\sum_{m=0}^{M-1} s_d(t) e^{j2\pi f_c\left(t-\left(\tau_d-\frac{((l-1)M+m-1)d}{c}sin\theta_d\right)-\frac{\alpha_{l,m}}{2\pi f_c}\right)} \\ &+ \sum_{k=1}^{K}\sum_{m=0}^{M-1} i_k(t) e^{j2\pi f_c\left(t-\left(\tau_k-\frac{((l-1)M+m-1)d}{c}sin\theta_k\right)-\frac{\alpha_{l,m}}{2\pi f_c}\right)} \\ &+ v_l(t), \end{aligned} \tag{1}$$

where d is the spacing between adjacent antenna array elements, assumed throughout this paper to be 0.5λ. τ_d and τ_k are the propagation delays from the desired signal emitter and k-th interference signal emitter, respectively, to a reference point which is assumed to be the first element on the array. c is the speed of light. Eq. (1) includes the phase difference $\alpha_{l,m}$ for the m-th phase shifter of the analog beamformer in the l-th sub-array. After the analog beamformer, the signals $\tilde{x}_l(t)$ with ($l = 1, \ldots, L$) pass through the L RF chains which include ADCs and down converters, resulting in the following

TABLE 1. Abbreviations index.

5G	Fifth-Generation	**LCMV**	Linearly Constrained Minimum Variance
ACO	Ant Colony Optimization	**Max-SLNR**	Maximizing Signal-to-Leakage-and-Noise Ratio
ADC	Analog-to-Digital Converter	**MIMO**	Multiple-Input Multiple-Output
ALO	Ant-Lion optimization	**MO**	Manifold Optimization
AltMin	Alternating Minimization	**MU**	Multi-User
AOA	Angle Of Arrival	**MVDR**	Minimum Variance Distortionless Response
APALS	Analog Phase Alignment By Linear Searching	**NBA**	Novel Bat Algorithm
APSO	Accelerated Particle Swarm Optimization	**PSACO**	Particle Swarm Ant Colony Optimization
AWGN	Additive White Gaussian Noise	**PSO**	Particle Swarm Optimization
BA	Bat Algorithm	**RABs**	Robust Adaptive Beamformers
CSI	Channel State Information	**RF**	Radio Frequency
CSO	Cat Swarm Optimization	**Root-MUSIC**	Root Multiple Signal Classification
DL	Diagonal Loading	**SA**	Simulated Annealing
DOA	Direction-of-arrival	**SCB**	Standard Capon Beamformer
GA	Genetic algorithm	**SDR**	Semidefinite Relaxation
GWO	Grey Wolf Optimizer	**SINR**	Signal-to-Interference-Plus-Noise Ratio
HAD	Hybrid Analog and Digital	**SLL**	sidelobe level
HADPA	Hybrid Analog And Digital Phase Alignment	**SMF**	Spatial Matched Filter
HDAPA	Hybrid Digital And Analog Phase Alignment	**SNR**	Signal-to-Noise-Ratio
I-BA	Improved Bat Algorithm	**SVD**	Singular Value Decomposition
IWO	Invasive Weed Optimization	**UAV**	Unmanned Aerial Vehicle
LAA	Linear Antenna Array	**WOA**	Whale Optimization Algorithm

baseband signal in a matrix-vector notation for all L subsets

$$\mathbf{x}(n) = F_{RF}^H A\mathbf{s}(n) + F_{RF}^H \mathbf{v}(n), \tag{2}$$

where

$$F_{RF} = diag\left(\mathbf{f}_1, \ldots, \ \mathbf{f}_l \ , \ldots, \mathbf{f}_L\right),$$
$$\mathbf{f}_l = \frac{1}{\sqrt{M}}\left[\exp\left(j\alpha_{1,l}\right), \ \exp\left(j\alpha_{2,l}\right), \ldots, \ \exp\left(j\alpha_{M,l}\right)\ \right]^T. \tag{3}$$

A matrix F_{RF} is the $N \times L$ phase shift matrix, $\mathbf{s}(n) = [s_d(n), i_1(n), \ \ldots, \ i_K(n)]^T$, $\mathbf{v}(n) = [v_1(n), \ v_2(n), \ \ldots, \ v_N(n)]^T$ is an AWGN, and A is $N \times (K+1)$ matrix of steering vectors $\mathbf{a}(\theta)$ which can be defined as

$$A = [\mathbf{a}(\theta_d), \ \mathbf{a}(\theta_1), \ldots, \ \mathbf{a}(\theta_K)], \tag{4}$$

where the column vector $\mathbf{a}(\theta)$ is called an array manifold, which can be given by

$$\mathbf{a}(\theta) = \left[1, \ e^{j\pi sin\theta}, \ldots \ , \ e^{j\pi(N-1)sin\theta}\right]^T \tag{5}$$

After the digital beamformer $\mathbf{f}_D \in \mathbb{C}^{N_{RF}\times 1}$, Eq. (2) becomes

$$y(n) = \mathbf{f}_D^H F_{RF}^H A\mathbf{s}(n) + \mathbf{f}_D^H F_{RF}^H \mathbf{v}(n) \tag{6}$$

Through the digital beamforming vector $\mathbf{f}_D$ we can control the amplitude, phase, or both.

$$\mathbf{f}_D = \left[a_1 e^{j\alpha_1}, \ a_2 e^{j\alpha_2}, \ \ldots \ , \ a_L e^{j\alpha_L}\right]^T \tag{7}$$

III. PROBLEM FORMULATION FOR SINR MAXIMIZATION

The input observation vector $\mathbf{x}(t)$, can also be formulated for all sub-arrays as

$$\begin{aligned}\mathbf{x}(t) &= \mathbf{a}(\theta_d)s_d(t) \ + \sum_{k=1}^{K}\mathbf{a}(\theta_k)\, i_k(t) + \mathbf{v}(t)\\ &= \ \mathbf{a}(\theta_d)s_d(t) \ + A_i\mathbf{i}(t) \ + \mathbf{v}(t)\\ &= \mathbf{x}_s(t) \ + \ \mathbf{x}_i(t) \ + \ \mathbf{v}(t),\end{aligned} \tag{8}$$

where A_i matrix constitutes of all steering vectors of interference signals, and $\mathbf{i}(t) = [i_1(t), \ i_2(t), \ \ldots, \ i_K(t)]^T$. In this work, we assume that all the signals are zero-mean and independent. Multiplying these signals by analog and digital beamformer weights and adding them together results in the following output

$$y(n) = \mathbf{f}_D^H F_{RF}^H(\mathbf{x}_s(n) + \mathbf{x}_i(n)) + \mathbf{f}_D^H F_{RF}^H \mathbf{v}(n). \tag{9}$$

The mean power of the desired signal p_d, the interference correlation matrix R_{ii}, and the noise correlation matrix R_{vv} (assuming independent noise signals) can be composed from the signals and noise samples at n time intervals, which are given by

$$\begin{aligned}p_d &= \mathbb{E}\left\{|s_d(n)|^2\right\},\\ R_{ii} &= \mathbb{E}\left\{\mathbf{i}(n)\,\mathbf{i}^H(n)\right\},\\ R_{vv} &= \mathbb{E}\left\{\mathbf{v}(n)\,\mathbf{v}^H(n)\right\} = p_v I_N.\end{aligned} \tag{10}$$

The SINR is given by dividing the power of the desired signal by the sum of powers of all interference and noise signals. The hybrid system output power for the signal of interest can be given by

$$\begin{aligned}\sigma_s^2 &= \mathbb{E}\left\{\left|\mathbf{f}_D^H F_{RF}^H \mathbf{x}_s(n)\right|^2\right\}\\ &= \mathbb{E}\left\{\left|\mathbf{f}_D^H F_{RF}^H \mathbf{a}(\theta_d)\, s_d(n)\right|^2\right\}\\ &= p_d\, \mathbf{f}_D^H F_{RF}^H \mathbf{a}(\theta_d)\, \mathbf{a}^H(\theta_d)\, F_{RF}\mathbf{f}_D.\end{aligned} \tag{11}$$

In the same context, we can derive the hybrid system output power for the unwanted signals as follows

$$\sigma_i^2 = \mathbf{f}_D^H F_{RF}^H A_i R_{ii} A_i^H F_{RF}\mathbf{f}_D, \tag{12}$$
$$\sigma_v^2 = p_v\, \mathbf{f}_D^H F_{RF}^H F_{RF}\mathbf{f}_D. \tag{13}$$

Therefore, the SINR is defined as

$$SINR = \frac{\sigma_s^2}{\sigma_i^2 + \sigma_v^2} = \frac{p_d\, \mathbf{f}_D^H F_{RF}^H \mathbf{a}(\theta_d)\, \mathbf{a}^H(\theta_d) F_{RF} \mathbf{f}_D}{\mathbf{f}_D^H F_{RF}^H A_i R_{ii} A_i^H F_{RF} \mathbf{f}_D + p_v\, \mathbf{f}_D^H F_{RF}^H F_{RF} \mathbf{f}_D}. \quad (14)$$

Our goal is to maximize the SINR. However, metaheuristic optimization algorithms usually look for the minima. Hence, the SINR maximization can equivalently be represented by the $(SINR)^{-1}$ minimization, as long as $SINR > 0$, which is achieved if any signal power from the desired signal is received at the receiver. Thus, the cost function (CF) can be given by the inverse of the SINR as follows

$$\underset{F_{RF},\, \mathbf{f}_D}{minimize}\ CF = \frac{\mathbf{f}_D^H F_{RF}^H A_i R_{ii} A_i^H F_{RF} \mathbf{f}_D + p_v \mathbf{f}_D^H F_{RF}^H F_{RF} \mathbf{f}_D}{p_d \left| \mathbf{f}_D^H F_{RF}^H \mathbf{a}(\theta_d) \right|^2},$$
$$s.t. \qquad \mathbf{f}_D^H F_{RF}^H \mathbf{a}(\theta_d) = 1. \quad (15)$$

Problem (15) is non-convex due to the fact that it is in the fractional form and the optimization variables are coupled. In order to efficiently solve this problem, we decompose it into two subproblems, and then solve them alternately. Specifically, for given analog beamformer F_{RF}, we solve problem (15) and obtain the digital beamformer vector $\mathbf{f}_D$. Then, for given $\mathbf{f}_D$, we sovle problem (15) and obtain the analog beamformer matrix F_{RF}.

A. DESIGN OF THE DIGITAL WEIGHT VECTOR

According to the unitary constraint, the denominator term $p_d \left| \mathbf{f}_D^H F_{RF}^H \mathbf{a}(\theta_d) \right|^2$ in (15) is constant. To proceed, we first rewrite problem (15) for given analog beamformer matrix F_{RF} as follows

$$\underset{\mathbf{f}_D}{minimize}\ \mathbf{f}_D^H F_{RF}^H R_{i+n} F_{RF} \mathbf{f}_D,$$
$$s.t. \qquad \mathbf{f}_D^H F_{RF}^H \mathbf{a}(\theta_d) = 1, \quad (16)$$

where

$$R_{i+v} = \sum_{k=1}^{K} P_k \mathbf{a}(\theta_k)\, \mathbf{a}^H(\theta_k) + p_v I_N. \quad (17)$$

We observe that, problem (16) is now a convex and the unitary constraint is linear. As such, the optimal solution can be obtained as will be shown in the next steps. If the actual covariance matrix R_{i+v} is well known, problem (16) can be solved using Lagrange's multiplier technique as

$$\mathbf{f}_D = \frac{R_{i+v}^{-1} F_{RF}^H \mathbf{a}(\theta_d)}{\left(F_{RF}^H \mathbf{a}(\theta_d)\right)^H R_{i+v}^{-1} F_{RF}^H \mathbf{a}(\theta_d)}. \quad (18)$$

Here, to calculate $\mathbf{f}_D$ we use the initial value of F_{RF} that makes the array main beam steers towards the direction of the desired signal. Since $\mathbf{f}_D^H F_{RF}^H \mathbf{a}(\theta_d) = 1$, the optimization problem (16) is equivalent to the following one

$$\underset{\mathbf{f}_D}{minimize}\ \mathbf{f}_D^H F_{RF}^H R_{i+v} F_{RF} \mathbf{f}_D + p_d \left| \mathbf{f}_D^H F_{RF}^H \mathbf{a}(\theta_d) \right|^2,$$
$$s.t. \qquad \mathbf{f}_D^H F_{RF}^H \mathbf{a}(\theta_d) = 1. \quad (19)$$

This because the second term in the optimization problem is constant, so, it will not have an effect on the problem solution. Problem (19) is still convex and can also be equivalently represented as

$$\underset{\mathbf{f}_D}{minimize}\ CF = \mathbf{f}_D^H F_{RF}^H \hat{R} F_{RF} \mathbf{f}_D,$$
$$s.t. \qquad \mathbf{f}_D^H F_{RF}^H \mathbf{a}(\theta_d) = 1, \quad (20)$$

where $\hat{R}$ is the estimated array covariance matrix, since a typical information about different signals may not be possible.

$$\hat{R} = \frac{1}{Q} \sum_{q=1}^{Q} \mathbf{x}(q)\, \mathbf{x}^H(q), \quad (21)$$

where Q is the snapshot size. The optimization problem (20) is with a convex cost function and a linear constraint. Hence, it is a convex optimization problem. The optimization problem (20) can efficiently be solved by Lagrange's multiplier like the solution of problem (16) as

$$\mathbf{f}_D = \frac{\hat{R}^{-1} F_{RF}^H \mathbf{a}(\theta_d)}{\left(F_{RF}^H \mathbf{a}(\theta_d)\right)^H \hat{R}^{-1} F_{RF}^H \mathbf{a}(\theta_d)}. \quad (22)$$

As Q increases, $\hat{R}$ will converge to the true covariance matrix. However, the convergence of the standard Capon beamformer (SCB) is very slow. To resolve this problem, a widely used diagonal loading method has been used in order to improve SCB performance. The diagonal loading technique can improve the performance of SCB by adding to the covariance matrix an identity matrix scaled by a real weight called diagonal loading level [50]. Assuming ξ is the proposed diagonal loading level, the new digital beamformer vector can be given by

$$\mathbf{f}_D = \frac{\left(\hat{R} + \xi I\right)^{-1} F_{RF}^H \mathbf{a}(\theta_d)}{\left(F_{RF}^H \mathbf{a}(\theta_d)\right)^H \left(\hat{R} + \xi I\right)^{-1} F_{RF}^H \mathbf{a}(\theta_d)}. \quad (23)$$

The diagonal loading level ξ has a considerable effect on the performance of SCB; therefore, several methods have been proposed to optimize the diagonal loading level. One of the most effective and simple methods is the spatial matched filter (SMF) method [49]. The loading level of the SMF is given by

$$\xi_{SMF} = \frac{1}{Q} \left\| \hat{\mathbf{a}}(\theta_d) X \right\|^2 = \hat{\mathbf{a}}^H(\theta_d) \hat{R}_x \hat{\mathbf{a}}(\theta_d), \quad (24)$$

where $\hat{\mathbf{a}}(\theta_d) = \frac{\mathbf{a}(\theta_d)}{\|\mathbf{a}(\theta_d)\|}$ is the normalized steering vector, and $\hat{R}_x = \frac{1}{Q} \mathbf{x}\mathbf{x}^H$ is the estimation covariance matrix of the received signal.

B. DESIGN OF THE ANALOG WEIGHT VECTORS

Given the digital beamformer vector $\mathbf{f}_D$, we solve problem (20) to obtain the analog beamformer matrix F_{RF} as follows

$$\begin{aligned} &\underset{\theta}{minimize} \;\; CF = \mathbf{f}_D^H F_{RF}^H \hat{R} F_{RF} \mathbf{f}_D, \\ &s.t. \qquad\quad \mathbf{f}_D^H F_{RF}^H \mathbf{a}(\theta_d) = 1, \end{aligned} \tag{25}$$

Problem (25) is a convex optimization problem since its objective function is convex and the constraint is linear. The digital beamformer vector $\mathbf{f}_D$ is given by (23). The angle θ is the searching angle in the range $\frac{-\pi}{2} \leq \theta \leq \frac{\pi}{2}$, which will be used to construct F_{RF}. Whereas, as shown in Eq. (3), the matrix F_{RF} can be built using the corresponding phase of the m-th antenna of subarray l, i.e., $\alpha_{m,l}$ as

$$\alpha_{m,l} = \frac{2\pi}{\lambda} \left((l-1)M + m + 1\right) dsin\theta. \tag{26}$$

By adjusting the value of θ in (26), we can minimize the cost function in (25). This can be done using the APALS with sufficiently fine grid of points in the above defined range of θ. To perform linear fine searching, we will use a small enough searching step size $\Delta\theta$, where the range of θ is divided into N_{step} sub-periods or points. Therefore, the angle θ in (26) is selected from the set, $\Theta \in \left\{-\frac{\pi}{2}, -\frac{\pi}{2} + \Delta\theta, \ \ldots\ ., \frac{\pi}{2}\right\}$. The optimization process of digital beamforming vector and analog beamforming matrix is done alternately until a stopping criterion is met as shown in algorithm 1.

C. OVERALL HYBRID BEAMFORMING ALGORITHM AND CONVERGENCE

Depending on the results presented in the previous subsections, the overall iterative hybrid algorithm (Algorithm 1) is proposed to solve problem (15). In each iteration, the digital beamformer $\mathbf{f}_D$ and analog beamformer F_{RF} are alternately optimized, by solving problem (20) and (25), respectively. The resulted solution in the t-th iteration is then used as the input of the next $(t+1)$th iteration. Next, we discuss the convergence analysis of Algorithm 1. First, returning to step 3 in Algorithm 1, where the optimal solution of Problem (20) is obtained for given F_{RF}^t, we get

$$CF\left(\mathbf{f}_D^t, \ F_{RF}^t\right) \geq \ CF\left(\mathbf{f}_D^{t+1}, \ F_{RF}^t\right), \tag{27}$$

which is right since problem (20) is solved optimally with given F_{RF}^t. Second, in step 4 of Algorithm 1, the optimal solution of Problem (25) is obtained for given $\mathbf{f}_D^{t+1}$, we have

$$CF\left(\mathbf{f}_D^{t+1}, \ F_{RF}^t\right) \geq \ CF\left(\mathbf{f}_D^{t+1}, \ F_{RF}^{t+1}\right) \geq \cdots \geq 0. \tag{28}$$

This holds since problem (25) is solved optimally with given $\mathbf{f}_D^{t+1}$, as seen in step 4 of Algorithm 1. Further, the minimization of the cost function of the inverse of SINR is lower bounded by zero. According to the above description, the proposed Algorithm 1 is convergent.

D. OPTIMAL SINR

Let $\mathbf{f}$ be a total beamforming vector, $\mathbf{f} = F_{RF}\mathbf{f}_D$. The weight vector $\mathbf{f}$ can be found from the maximum of the SINR, hence, Eq. (14) can be rewritten as

$$SINR = \frac{p_d \, \mathbf{f}^H \mathbf{a}\left(\theta_d\right) \mathbf{a}^H\left(\theta_d\right) \mathbf{f}}{\mathbf{f}^H R_{i+v} \mathbf{f}}. \tag{29}$$

Problem (27) can be formed the same as (16), therefore, the optimal weight vector is given by

$$\mathbf{f}_{opt} = \frac{R_{i+v}^{-1} \mathbf{a}\left(\theta_d\right)}{\mathbf{a}^H\left(\theta_d\right) R_{i+v}^{-1} \mathbf{a}\left(\theta_d\right)}. \tag{30}$$

Inserting (30) into (29), we obtain the optimal SINR, $SINR_{opt} = p_d \mathbf{a}\left(\theta_d\right)^H R_{i+v}^{-1} \mathbf{a}\left(\theta_d\right)$, which gives an upper bound of the output SINR.

E. PARTIALLY-CONNECTED HAD SYSTEM DESIGN FOR MULTIPLE DATA STREAMS

The previous solution was for one data stream, i.e., one received desired signal. However, we can easily extend our system to support multiple data streams using the same methods. Considering one desired signal $s_{d,l}(t)$ per subarray, $l \in \{1, \ \ldots\ , L\}$. As such, the digital beamformer $F_D \in \mathbb{C}^{L \times N_s}$ is used to demodulate the N_s received data streams, where N_s is assumed in this paper to be equal to the number of RF chains. The digital beamformer matrix can be written as

$$F_D = \left[\mathbf{f}_{D,1}, \ \mathbf{f}_{D,2}, \ \ldots, \ \mathbf{f}_{D,l}, \ldots, \ \mathbf{f}_{D,L}\right], \tag{31}$$

where $\mathbf{f}_{D,l}$ is a digital beamformer vector for the l-th subarray. The estimated l-th data stream $\hat{s}_{d,l}$ received at the l-th sub-array can be given by

$$\begin{aligned} \hat{s}_{d,l} = &\mathbf{f}_{D,l}^H F_{RF}^H \mathbf{a}(\theta_{d,l}) s_{d,l} \\ &+ \sum_{i=1, i\neq l}^{N_s} \mathbf{f}_{D,l}^H F_{RF}^H \mathbf{a}(\theta_{d,i}) s_{d,i} + \mathbf{f}_{D,l}^H F_{RF}^H \mathbf{v}. \end{aligned} \tag{32}$$

Using the same derivation strategies as in (10)-(13), the SINR of the l-th data stream ($SINR_l$) can be represented as

$$SINR_l = \frac{p_d \left|\mathbf{f}_{D,l}^H F_{RF}^H \mathbf{a}(\theta_{d,l})\right|^2}{\sum_{i=1, i\neq l}^{N_s} p_i \left|\mathbf{f}_{D,l}^H F_{RF}^H \mathbf{a}(\theta_{d,i})\right|^2 + p_v \left\|\mathbf{f}_{D,l}^H F_{RF}^H\right\|^2}. \tag{33}$$

The achievable sum-rate of the partially-connected HAD receiver is given by

$$R = \sum_{l=1}^{N_s} log_2\left(1 + SINR_l\right). \tag{34}$$

As mentioned before, our goal is to maximize the SINR. Here, in order to solve this maximization problem, we decompose it into L subproblems, and then solve them separately, i,e., maximize the $SINR_l$, $l \in \{1, \ \ldots\ , L\}$. Therefore, take these into account, and follow the same derivation steps and tactics

Algorithm 1 Proposed DL and I-BA Based HAD Beamformers for Single Data Stream

Input: 1: Initializing F_{RF};
2: **repeat**
3: Solve (20) with given F_{RF} and obtain $\mathbf{f}_D$;
4: Solve (25) with given $\mathbf{f}_D$ and obtain F_{RF};
5: **until** a stopping criterion is met.
Output: $\mathbf{f}_D$, F_{RF}.

as in (15)-(19), problem (20) can be reformulated for multiple data streams system as follows

$$\begin{aligned} &\underset{\mathbf{f}_{D,l},F_{RF}}{minimize} \ \mathbf{f}_{D,l}^H F_{RF}^H \hat{R} F_{RF} \mathbf{f}_{D,l}, \\ &s.t. \qquad \mathbf{f}_{D,l}^H F_{RF}^H \mathbf{a}\left(\theta_{d,l}\right) = 1. \end{aligned} \tag{35}$$

For a given analog beamformer matrix F_{RF}, problem (35) will have the same solution for $\mathbf{f}_{D,l}$ as in (23).

Given the digital beamformer vectors $\mathbf{f}_{D,l}$, $l \in \{1, \ldots, L\}$, the analog beamformer matrix construction problem can also be divided into L sub-problems. Each sub-problems can be solved using the same optimization method used with problem (25), i.e., linear searching. Therefore, the optimization problem given in (35) is now used to solve for analog beamformer using the search angle θ_l for l-th subarray. For each searching round we optimize one $\mathbf{f}_l$ vector from the analog beamforming matrix F_{RF} given in (3). The remaining vectors are fixed to the initial values and the vectors previously optimized. The initial values of F_{RF} vectors are chosen so as to make the subarrays directed toward the DOAs of the desired signals. This process is done alternately until a stopping criterion is met as shown in algorithm 2.

IV. PROPOSED METAHEURISTIC OPTIMIZATION ALGORITHM

The previously employed DL methods take advantage of closed-form solutions for the given problems. However, metaheuristic and stochastic techniques have been observed as more flexible and efficient. Metaheuristic algorithms have a powerful ability for antenna array patterns synthesis such as null steering. Unlike metaheuristic approaches, which have global search ability, deterministic optimization methods are very sensitive to the initial points [13]. More importantly, DL techniques are complex weights' methods, resulting in an expensive receiver. As such, they are impractical, especially for battery-powered applications due to the need of employing both phase shifters and attenuators. Consequently, we propose an efficient metaheuristic optimization algorithm in order to optimize the digital beamforming weights using only the phase; Whereas, digital beamforming vector can be adjusted using amplitude only (i. e., $a_1, a_2, \ldots, a_L$), phase only (i. e., $\alpha_1, \alpha_2, \ldots, \alpha_L$), or both (i. e., complex weights) as shown in Eq. (7).

The BA is inspired from the advanced echolocation capability of bats used to sense distances in order to avoid barrier

Algorithm 2 Proposed DL and I-BA Based HAD Beamformers for Multiple Data Streams

Input: 1: Initializing F_{RF};
2: **repeat**
3: **for** each subarray **do**
4: Solve (33) with given F_{RF} and obtain $\mathbf{f}_{D,l}$;
5: Solve (33) with given $\mathbf{f}_{D,l}$ and obtain F_{RF};
6: **end**
7: **until** a stopping criterion is met.
Output: F_D, F_{RF}.

and detect prey. It is a promising optimization algorithm that is characterized by robustness, accuracy, and fast convergence compared to its predecessors such as genetic algorithm and PSO. Further details about the BA can be found in [10], [51] and other references therein. The BA had received a number of improvement attempts in recent years in order to address the algorithm's shortcomings such as unstable results and being trapped in the local minima [45]–[47]. In this paper we adopt the novel BA (NBA) proposed by Meng *et al.* [46]. In addition, more refinement has been made in order to improve stability by tuning the inertia weight using random variables to help the algorithm easily skip out of the local minima [45].

A. IMPROVED BAT ALGORITHM

The I-BA optimizes a problem by iteratively searching the candidate solutions in the search-space toward the best solution. For our problem, the I-BA will be used to optimize (20) by iteratively searching the entire search-space, which are the phases of the digital beamforming in the range $-\frac{\pi}{2} \leq \alpha_l \leq \frac{\pi}{2}$, $l \in \{1, \ldots, L\}$. In each iteration of I-BA, the velocity and position of each Bat are adjusted toward the best position. For our problem the phases of the digital beamforming vector $\mathbf{f}_D$ need to be optimized, i.e., $\alpha_1, \alpha_2, \ldots, \alpha_L$. First, we initialise Z Bats (swarm size) with random positions $\alpha_1^{(0)}, \alpha_2^{(0)}, \ldots, \alpha_L^{(0)}$. The position of the Bat is used to evaluate (20), which is solved for $\mathbf{f}_D$. Secondly, the bats' habitat selection depends on a stochastic decision. If a uniform random number $R \in [0,\ 1]$ is less than the threshold of the selection $P \in [0,\ 1]$, bats positions can be represented as

$$\alpha_{ij}^{t+1} = \begin{cases} g_j^t + \Phi * \left| m_j^t - \alpha_{ij}^t \right| * ln\left(\frac{1}{u_{ij}}\right), & if\ rand_j() < P, \\ g_j^t - \Phi * \left| m_j^t - \alpha_{ij}^t \right| * ln\left(\frac{1}{u_{ij}}\right), & otherwise, \end{cases} \tag{36}$$

where α_{ij}^t is the Z bats' positions in a D-dimensional space, $i \in [1, \ldots, Z]$, $j \in [1, \ldots, D]$. Φ is the contraction - expansion coefficient. g_j^t and m_j^t are the global best position and the mean of the individual's best position in a D-dimensional space at time step t, respectively. Finally, u_{ij} is a number uniformly distributed in the range between 0 and 1. On the other side, if R is greater than or equal to P, bats positions mathematical model can be represented as

follows

$$f_{i,j} = f_{min} + (f_{max} - f_{min}) * rand\ (0,\ 1)\,, \tag{37}$$

$$f_{i,j}^{'} = \frac{\left(c + v_{i,j}^{t}\right)}{c + v_{i,j}^{t}} * f_{i,j} * \left(1 + C_i * \frac{\left(g_j^t - \alpha_{i,j}^t\right)}{\left|g_j^t - \alpha_{i,j}^t\right| + \varepsilon}\right), \tag{38}$$

$$v_{i,j}^{t+1} = w * v_{i,j}^{t} + (g_j^t - \alpha_{i,j}^t) * f_{i,j}, \tag{39}$$

$$\alpha_{i,j}^{t+1} = \alpha_{i,j}^{t} + v_{i,j}^{t}, \tag{40}$$

In the BA, bats fly randomly at position α_i^t with velocity v_i^t, loudness Λ_i^t, frequency f_i in a range $[f_{min},\ f_{max}]$, and the pulse rate of emission r_i^t in the range of [0, 1]. C is a positive number representing the compensation rates, ε is the smallest constant number in the computer used to avoid zero-division error, c is the speed of signal in the air ($c = 340\ m/s$), and w is an inertia weight parameter that can be adjusted in order to improve the stability of the algorithm by quickly jump out of the local minima, which is given by

$$w = \mu_{min} + (\mu_{max} - \mu_{min}) * rand() + \sigma \times randn(), \tag{41}$$

where μ_{min}, μ_{max} are the minimum and maximum factor of the stochastic inertia weight, respectively. $rand()$, $randn()$ are the random number between 0 and 1, and the random number of standard normal distribution, respectively. σ is the deviation between the stochastic inertia weight and its mean. Finally, with regard to local search, the local generation new position for each bat can be represented as follows

$$if\ (randn\,(0,\ 1) > r_i), \tag{42}$$

$$\alpha_{i,j}^{t+1} = g_j^t * \left(1 + randn\left(0,\ \sigma^2\right)\right), \tag{43}$$

$$\sigma^2 = \left|\Lambda_i^t - \Lambda_{mean}^t\right| + \varepsilon, \tag{44}$$

where $randn(0, \sigma^2)$ is a Gaussian distribution with 0 mean and variance σ^2. Λ_{mean}^t is the average loudness of all bats at time step t. As iteration progress, the loudness Λ_i and the rate r_i of emission pulse can be updated by

$$\Lambda_i^{t+1} = \varsigma\Lambda_i^t, \quad r_i^{t+1} = r_i^0[1 - \exp(-\gamma t)\,, \tag{45}$$

where ς and γ are constants ($0 < \varsigma < 1,\ \gamma > 0$), which can be tuned experimentally. Based on the above description, the basic steps of the I-BA are summarized in algorithm 3.

B. COMPLEXITY ANALYSIS

The I-BA involves as high complexity as all other metaheuristic techniques. The computational complexity of I-BA' pseudo-code itself is $O\,(ZT_{max})$. As shown in Table 2, the complexity of the cost function for the proposed I-BA is scaled with the maximum number of iterations (T_{max}) multiplied by swarm size (Z). The smaller the number of maximum iterations and swarm size, the closer the complexity of the I-BA-APALS with the DL-SMF-APALS, and DL-APALS hybrid algorithms. Table 2 also presents the comparison of the I-BA complexity with the optimal and fully-digital algorithms. N_{ite} is the maximum alternate iterations in Algorithm 1.

TABLE 2. Complexity comparison.

Algorithms	Computational Complexity
Optimal	$O(N^3+N^2)$.
SCB	$O(N^3+NQ(N+K))$.
DL	$O(N^3+NQ(N+K))$.
DL-APALS	$O((L^2(L+Q)+LK(Q+N)+(N^2+NL)N_{step})N_{ite})$.
SMF-APALS	$O((L^2(L+Q)+LK(Q+N)+NQ(N+1)+(N^2+NL)N_{step})N_{ite})$.
I-BA-APALS	$O(((N^2(Q+1)+NQ)ZT_{max}+(N^2+NL)N_{step})N_{ite})$.

Algorithm 3 Proposed I-BA Based Digital Beamformer

Input: The bat population size Z; Maximum number of iterations T_{max}; Desired and interferences angles θ_d, θ_j; Parameters of original BA, ς, γ, f_{min}, f_{max}, Λ_o, r_o; Parameters of I-BA, P, C, Φ, G, σ.
Initialize the digital beamformer parameters $\alpha_1, \alpha_2, \ldots, \alpha_L$, and calculate cost function of each bat by (20)

```
for (i < T_max) do
    if (rand (0, 1) < P) then
        Generating new solutions using Eq. (36).
    else
        Generating new solutions using Eqs. (37)-(41).
    end
    if (rand > r_i) then
        Generating a local solution around the selected
        best solution using Eqs. (42)-(44).
    end
    Select a solution among the best solutions.
    Updating new solutions, the loudness and pulse
    emission rate using Eq. (45).
    Ranking the bats and finding the current best g^t.
    if the current best does not improve in G time step
    then
        Re-initialize the loudness Λ_i and set temporary
        pulse rates r_i as a uniform random number
        between [0.85, 0.9].
    end
    i = i + 1
end
```

Output: Digital beamforming vector $\mathbf{f}_D$.

V. SIMULATION RESULTS

In this section, we evaluate the performance of the DL-APALS, DL-SMF-APALS, and I-BA-APALS hybrid algorithms and compare them with the fully-digital SCB [52] and DL [48] optimization algorithms. A partially-connected HAD beamforming receiver with $L = 4$ RF chains is adopted in the simulations. The simulation parameters used by the I-BA and other metaheuristic algorithms are presented in Table 3. Unless otherwise stated, the other parameters

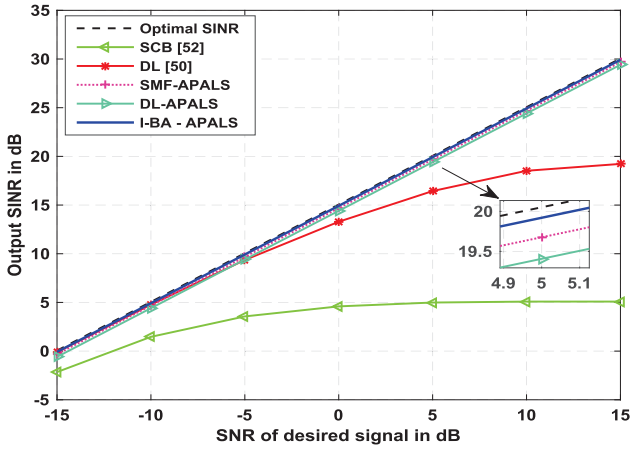

FIGURE 2. Output SINR comparison of DL techniques and proposed I-BA in the absence of mismatch, $N = 32$, and $Q = 128$.

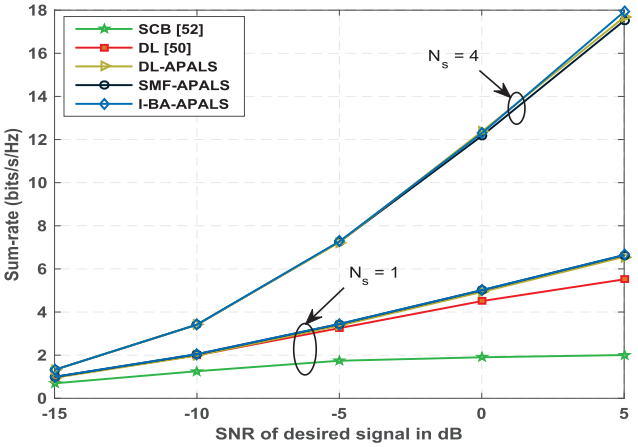

FIGURE 3. Sum-rate variations with different algorithms and data streams, $N = 32$, and $Q = 128$.

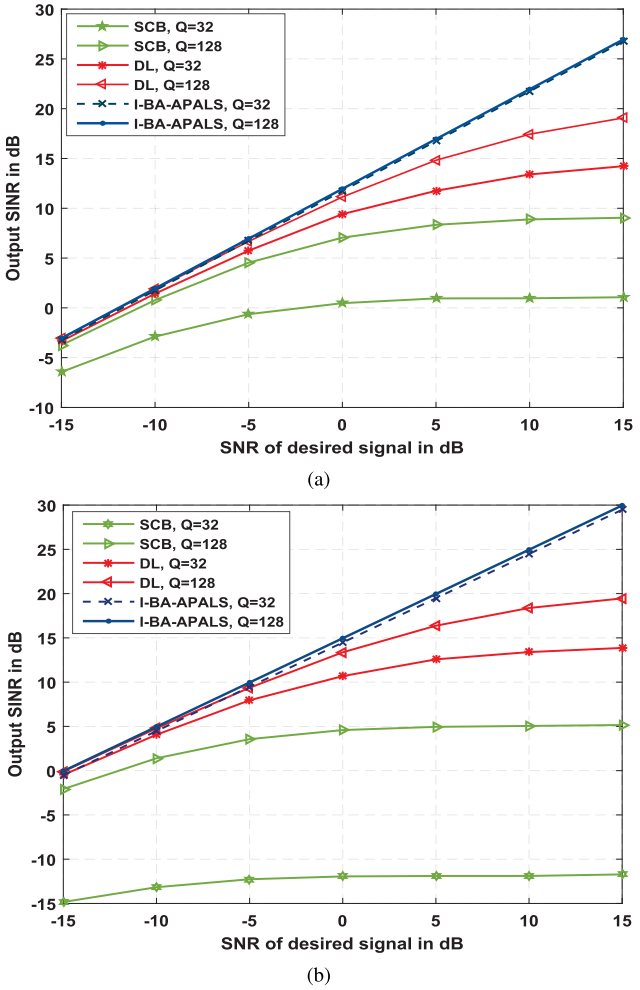

FIGURE 4. The effects of snapshots size on the output SINR in the absence of mismatch, (a) $N = 16$, (b) $N = 32$.

are set as: diagonal loading level $\xi = 30$, half-wavelength antenna spacing between adjacent elements, the antenna array receives the desired signal from angle $\theta_d = 0^o$, and two interference signals arriving from angles $\theta_k = 60^o, \ -30^o$. The SNR of the interference signals (SNR_i) is assumed to be 15 dB.

Fig. 2 presents the output SINR versus input SNR of the desired signal (SNR_d). In this examination, Q is set to be 128 snapshots and N to be 32-elements. Fig. 2 compares the proposed hybrid algorithms based on RAB techniques i.e., DL-APALS and SMF-APALS, and I-BA i.e., I-BA-APALS with fully-digital methods. Observing Fig. 2, we notice that our proposed hybrid algorithm based on I-BA has a better performance compared to all other techniques. The hybrid I-BA-APALS has the best performance which is highly close to the optimal, followed by the SMF-APALS with a very close performance. As can be seen, the traditional SCB and DL methods have very poor performance for higher SNR_d.

Fig. 3 plots the sum-rate achieved versus the SNR_d. For multiple data streams, 4 data streams are considered (one data stream per subarray), where we use 4 RF chains in this test. As shown, the rate of the system increases as the SNR improves. The hybrid I-BA-APALS algorithm has always better achievable rate compared to other hybrid and conventional algorithms. However, all proposed hybrid algorithms have very close performance. It is worth mentioning, due to the alternating optimization process of digital and analog beamformers as shown in Algorithm 2, the global optimal may not be achieved, which may result in a bit less rate performance.

Fig. 4 (a) and Fig. 4 (b) present the curves of the output SINR versus input SNR of the desired signal for the antenna array size equaling 16-elements and 32-elements, respectively. These figures investigate the effect of snapshots size into the performance of different algorithms. As shown, while the performance is improved considerably as the number of snapshots increased for SCB and DL techniques, there is very little effect on the performance of our proposed algorithm. On the other hand, observing these figures, we found that the SCB method has very low performance compared with our proposed I-BA-APALS hybrid algorithm and DL technique, as expected. The significant degradation in the performance

TABLE 3. Parameters used for different algorithms.

Algorithm	Parameters
PSO	*Inertia weight* $(w) \in [0.4,\ 0.9]$, *acceleration factor*$(C_1 = 0.5, C_2 = 0)$.
BA	$\varsigma = \gamma = 0.9$, $f_{min} = 0$, $f_{max} = 2$, $\Lambda_o \in [0,\ 2]$, $r_o \in [0,\ 1]$.
Improved-BA	$\varsigma = \gamma = 0.9$, $f_{min} = 0$, $f_{max} = 1.5$, $\Lambda_o \in [0,\ 2]$, $r_o \in [0,\ 1]$, $G = 2$, $P \in [0.5,\ 0.9]$, $C \in [0.1,\ 0.9]$, $\Phi \in [0.5,\ 1]$, $\mu_{min} = 0.4$, $\mu_{max} = 0.9$, $\sigma = 0.2$.

TABLE 4. Comparison between the results of null depth for different algorithms with 16-elements antenna array and 128 snapshots.

Algorithm	Null Depth in dB			Optimized angle (θ) [rad.]	Optimized digital beamformer phases $(\alpha_1,\ \alpha_2,\ \alpha_3,\ \alpha_4)$ [rad.]
	-30^o	15^o	60^o		
SCB [47]	-17.8696	-18.4928	-22.4583	–	–
DL [44]	-21.0869	-18.8732	-19.7341	–	–
DL-APALS	-50.8835	-22.4327	-20.8203	3.6732e-06	–
SMF-APALS	-48.5230	-20.7392	-20.8587	-6.3268e-06	–
PSO-APALS	-50.8951	-48.4151	-52.4867	3.6732e-06	-0.0764 0.0344 -0.3020 -0.1912
BA-APALS	-50.8951	-47.7281	-49.0414	3.6732e-06	-0.2507 -0.1398 -0.4762 -0.3655
I-BA-APALS	-50.8951	-48.4527	-52.5818	3.6732e-06	-0.0718 0.0391 -0.2973 -0.1865

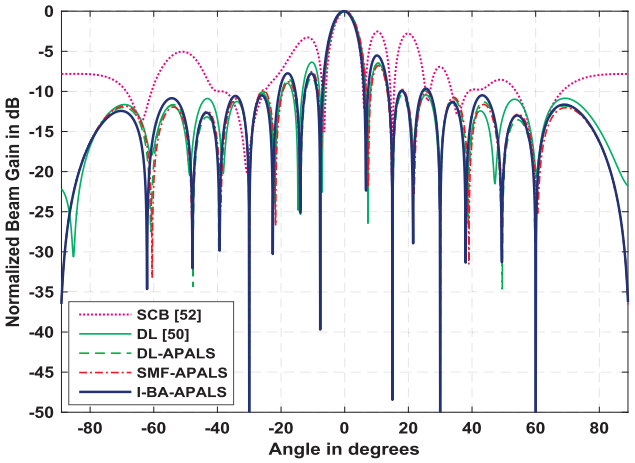

FIGURE 5. Radiation pattern with nulls placement at -30^o, 15^o, and 60^o with $N = 16$ and $Q = 128$.

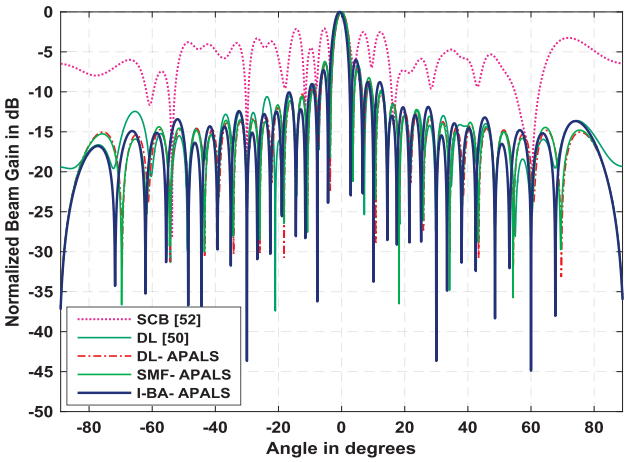

FIGURE 6. Radiation pattern with nulls placement at -30^o, and 60^o with $N = 32$ and $Q = 128$.

of the SCB method shown in Fig. 4 is because of the growing difference between the estimated array covariance matrix $\hat{R}$ and the true covariance matrix as N increases. For the SNR_d less than -5dB, we noticed that the DL technique and our proposed algorithm have almost close performance. However, for higher values of the SNR_d, the performance of our proposed algorithm is significantly better than the DL technique. Therefore, our proposed algorithm has a better ability for interference suppression.

To examine the performance of the hybrid and fully-digital algorithms in null steering, Fig. 5 and Fig. 6 show the optimized beamforming gains for 16 and 32 antenna array elements, respectively. The SNR_d and SNR_i are chosen to be -5dB and 15dB, respectively. The design in Fig. 5 optimizes the radiation patterns of a ULA with three null steering at -30^o, 15^o, 60^o, while two null at -30^o, 60^o are considered in Fig. 6. The resulted deep null, optimized angle of the analog beamforming, and phases of the digital beamforming are given in Table 4 and Table 5. As can be seen clearly from these tables, hybrid algorithms based on the proposed I-BA and other metaheuristic techniques have better ability to put deep null at the predefined locations of interference signals compared to RAB methods. The I-BA-APALS has achieved the deepest null of at least -43 dB at all desired null directions. As can be shown, hybrid algorithms based on RAB methods, i.e., DL-APALS and SMF-APALS have a weak ability to mitigate more than one interference signal. On the other hand, as can be shown, the optimized angles of the analog beamformers are almost the same for all hybrid algorithms, which means that the analog beamforming matrix has little effect on the null steering. It mainly directs the main beam towards the desired direction.

a: CONVERGENCE CHARACTERISTICS

Fig. 7 shows comparative convergence characteristic graphs obtained using BA, PSO, and proposed algorithm. The population size is set to be equal 40 for all algorithms and cases. All algorithms are used to solve the objective function given

TABLE 5. Comparison between the results of null depth for different algorithms with 32-elements antenna array and 128 snapshots.

Algorithm	Null Depth in dB		Optimized angle (θ)	Optimized digital beamformer phases (α_1, α_2, α_3, α_4)			
	-30^o	60^o	[rad.]	[rad.]			
SCB [47]	-20.6373	-25.9167	–	–			
DL [44]	-24.8710	-23.0476	–	–			
DL-APALS	-43.4445	-19.3077	2.0367e-05	–			
SMF-APALS	-43.4502	-22.8479	2.0367e-05	–			
PSO-APALS	-43.5743	-44.8705	2.0367e-05	0.1005	-0.1491	-0.3747	-0.5762
BA-APALS	-43.4877	-44.8421	2.0367e-05	-1.2033	-1.4288	-1.4181	-1.5437
I-BA-APALS	-43.6621	-44.8774	2.0367e-05	-0.0095	-0.2351	-0.6238	-0.8493

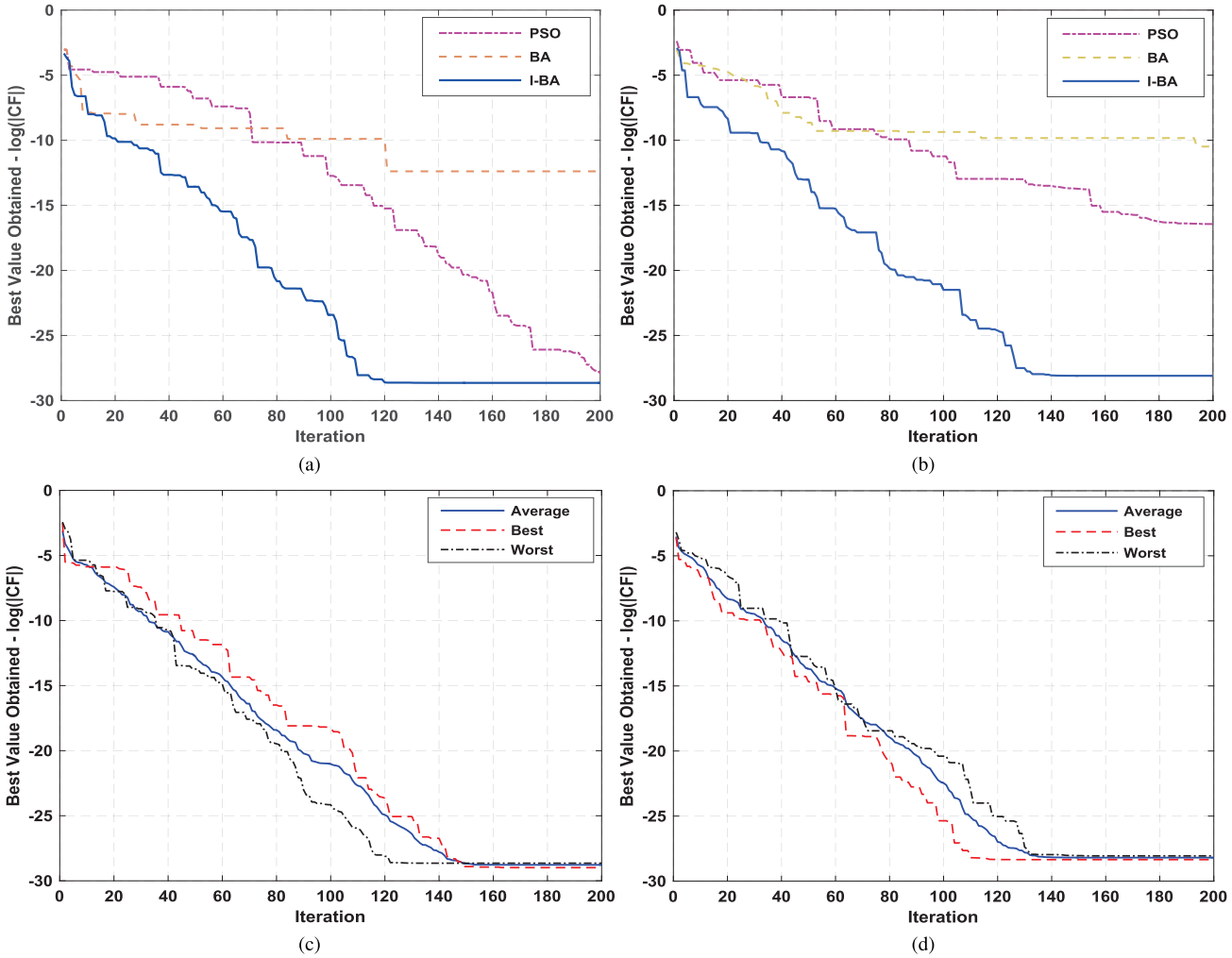

FIGURE 7. Convergence characteristics curves for varying SNR_d, N, and Q, (a) $N = 16$, $Q = 128$, $SNR_d = 0$, (b) N = 32, $Q = 200$, $SNR_d = -15$, (c) Convergence curves of I-BA, $N = 16$, $Q = 128$, $SNR_i = 30$, $SNR_d = -15$, (d) Convergence curves of I-BA, N = 32, $Q = 200$, $SNR_i = 30$, $SNR_d = 0$.

in (20) with a different number of antennas, snapshot size, SNR_i, and SNR_d. In Fig. 7 (a) and Fig. 7 (b), the number of antenna array elements are set to be 16 and 32, whereas, the snapshots size are set to be 128 and 200, respectively. The SNR_i is chosen to be 15dB, and the SNR_d is set to be 0dB and -15dB, respectively. Observing these curves, it is shown that the BA gets local optimal solution early in both figures; however, our proposed algorithm has a better ability to jump from local minima in both cases. Although PSO has a close optimal solution to I-BA in Fig. 7 (a), it has poor performance for higher antenna array size. The comparison of average convergence curves of the proposed algorithm is illustrated in Fig. 7 (c) and Fig. 7 (d) for 20 runs, which shows a quite good stability.

Fig. 8 illustrates the effect of antenna array size on the performance of the hybrid beamformer we are proposed. From Fig. 8, it is shown that the performance of the proposed beamformer based on I-BA-APALS is gradually improved with increased number of antennas. As noticed from the curves, for our proposed algorithm, the various values of the

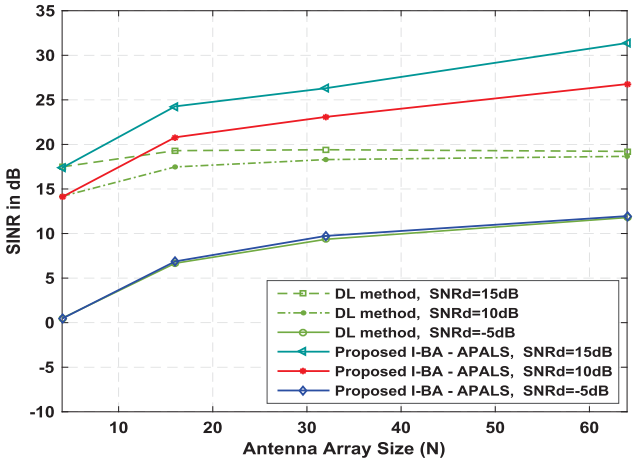

FIGURE 8. The effects of varying the number of antennas into the SINR when the SNR of interference signals is fixed ($SNR_i = 15$ dB) for different SNR_d and snapshots = 128.

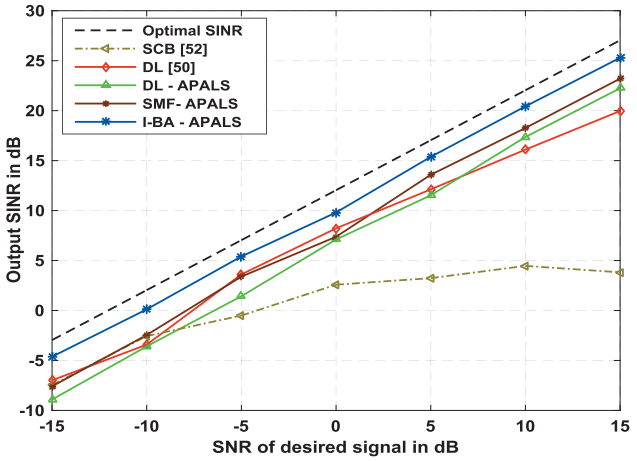

FIGURE 9. Output SINR versus input SNR of the desired signal in the presence of DOA mismatches, $N = 16$, and $Q = 200$.

received SNR of the desired signal have a significant impact on the performance. We can see a marked improvement on the performance for our proposed algorithm as SNR_d increased, and less impact on the performance of DL method for higher values of SNR_d.

b: THE IMPACT OF DOA MISMATCHES

Finally, Fig. 9 examines the effect of DOA mismatch into the performance of the proposed robust adaptive methods. The number of antenna array elements and snapshot size are set to be 16 and 200, respectively. The maximum estimation DOA angle mismatch is chosen to be 3^o. Fig. 9 further compares the performance of the classic SCB, and DL methods with the hybrid I-BA-APALS, DL-APALS, and SMF-APALS proposed techniques in the presence of DOA mismatch. As can be seen, the proposed I-BA-APALS shows better robustness performance to the DOA mismatch followed by SMF-APALS with close performance. This is because the proposed I-BA-APALS has good flexibility, therefore, it has a less impact by the DOA mismatch, and snapshot size.

VI. CONCLUSION

In this paper, we have proposed a hybrid beamforming system based on three hybrid adaptive beamforming techniques, namely, DL-APALS, SMF-APALS, and I-BA-APALS, with the objective of maximizing the SINR. The first two methods use only a linear searching to optimize the analog beamforming vectors, where the optimum digital beamforming vector is obtained by closed-form solution. In the last hybrid scheme, we further proposed an efficient nature-inspired optimization technique, that is, I-BA with the aim of optimizing the digital beamforming vector, which gave better global optima, convergence speed, and stability performance as compared to BA and PSO. With the aid of simulation and analysis, we found that the performance of the traditional adaptive beamformers, i.e., SCB, and DL techniques have serious degradation when the input SNR of the desired signal is large. By combining the DL, SMF, and I-BA methods with linear searching scheme to optimize the total beamforming vector, we got a better performance by I-BA-APALS in terms of output SINR, null depth, and robustness against DOA mismatch followed by SMF-APALS. On the other hand, since the I-BA-APALS depends on the phase-only as a controlling parameter, resulting in an inexpensive receiver that makes it convenient for practical implementation. This makes our proposed beamformer appropriate for many future applications that are likely to be susceptible to interference such as future 5G wireless cellular communication systems and battery-powered devices, e.g. unmanned aerial vehicles (UAVs) and other Internet of things (IoT) systems.

REFERENCES

[1] J. S. Blogh and L. Hanzo, *Third-Generation Systems and Intelligent Wireless Networking: Smart Antennas and Adaptive Modulation*. New York, NY, USA: Wiley, 2002.
[2] R. N. Biswas, A. Saha, S. K. Mitra, and M. K. Naskar, "Realization of PSO-based adaptive beamforming algorithm for smart antennas," in *Advances Nature-Inspired Computing Applications*, 1st ed. Cham, Switzerland: Springer, 2019, pp. 135–136.
[3] F. Shu, Y. Qin, T. Liu, L. Gui, Y. Zhang, J. Li, and Z. Han, "Low-complexity and high-resolution DOA estimation for hybrid analog and digital massive MIMO receive array," *IEEE Trans. Commun.*, vol. 66, no. 6, pp. 2487–2501, Feb. 2018.
[4] S. Han, C.-L. I, Z. Xu, and C. Rowell, "Large-scale antenna systems with hybrid analog and digital beamforming for millimeter wave 5G," *IEEE Commun. Mag.*, vol. 53, no. 1, pp. 186–194, Jan. 2015.
[5] O. El Ayach, S. Rajagopal, S. Abu-Surra, Z. Pi, and R. W. Heath, Jr., "Spatially sparse precoding in millimeter wave MIMO systems," *IEEE Trans. Wireless Commun.*, vol. 13, no. 3, pp. 1499–1513, Mar. 2014.
[6] X. Zhang, A. F. Molisch, and S.-Y. Kung, "Variable-phase-shift-based RF-baseband codesign for MIMO antenna selection," *IEEE Trans. Signal Process.*, vol. 53, no. 11, pp. 4091–4103, Nov. 2005.
[7] E. Ali, M. Ismail, R. Nordin, and N. F. Abdulah, "Beamforming techniques for massive MIMO systems in 5G: Overview, classification, and trends for future research," *Frontiers Inf. Technol. Electron. Eng.*, vol. 18, no. 6, pp. 753–772, 2017.
[8] O. El Ayach, R. W. Heath, Jr., S. Rajagopal, and Z. Pi, "Multimode precoding in millimeter wave MIMO transmitters with multiple antenna sub-arrays," in *Proc. IEEE Global Telecommun. Conf. (GLOBECOM)*, Atlanta, GA, USA, Dec. 2013, pp. 3476–3480.
[9] K. R. Subhashini and J. K. Satapathy, "Development of an enhanced ant lion optimization algorithm and its application in antenna array synthesis," *Appl. Soft Comput.*, vol. 59, pp. 153–173, Oct. 2017.
[10] T. Van Luyen and T. V. B. Giang, "Interference suppression of ULA antennas by phase-only control using bat algorithm," *IEEE Antennas Wireless Propag. Lett.*, vol. 16, pp. 3038–3042, 2017.

[11] U. Singh and R. Salgotra, "Synthesis of linear antenna array using flower pollination algorithm," *Neural Comput. Appl.*, vol. 29, no. 2, pp. 435–445, Jan. 2018.
[12] P. Saxena and A. Kothari, "Optimal pattern synthesis of linear antenna array using grey wolf optimization algorithm," *Int. J. Antennas Propag.*, vol. 2016, Mar. 2016, Art. no. 1205970.
[13] P. Saxena and A. Kothari, "Ant lion optimization algorithm to control side lobe level and null depths in linear antenna arrays," *AEU Int. J. Electron. Commun.*, vol. 70, no. 9, pp. 1339–1349, 2016.
[14] A. Fraser and D. Burnell, *Computer Models in Genetics*. New York, NY, USA: McGraw-Hill, 1970.
[15] R. L. Haupt, "Thinned arrays using genetic algorithms," *IEEE Trans. Antennas Propag.*, vol. 42, no. 7, pp. 993–999, Jul. 1994.
[16] R. Eberhart and J. Kennedy, "A new optimizer using particle swarm theory," in *Proc. 6th Int. Symp. Micro (MHS)*, Nagoya, Japan, Oct. 1995, pp. 39–43.
[17] M. M. Khodier and C. G. Christodoulou, "Linear array geometry synthesis with minimum sidelobe level and null control using particle swarm optimization," *IEEE Trans. Antennas Propag.*, vol. 53, no. 8, pp. 2674–2679, Aug. 2005.
[18] N. Jin and Y. Rahmat-Samii, "Advances in particle swarm optimization for antenna designs: Real-number, binary, single-objective and multiobjective implementations," *IEEE Trans. Antennas Propag.*, vol. 55, no. 3, pp. 556–567, Mar. 2007.
[19] C. Zhang, X. Fu, L. Leo, S. Peng, and M. Xie, "Synthesis of broadside linear aperiodic arrays with sidelobe suppression and null steering using whale optimization algorithm," *IEEE Antennas Wireless Propag. Lett.*, vol. 17, no. 2, pp. 347–350, Jan. 2018.
[20] V. Murino, A. Trucco, and C. S. Regazzoni, "Synthesis of unequally spaced arrays by simulated annealing," *IEEE Trans. Signal Process.*, vol. 44, no. 1, pp. 119–122, Jan. 1996.
[21] G. Ram, D. Mandal, R. Kar, and S. P. Ghoshal, "Cat swarm optimization as applied to time-modulated concentric circular antenna array: Analysis and comparison with other stochastic optimization methods," *IEEE Trans. Antennas Propag.*, vol. 63, no. 9, pp. 4180–4183, Sep. 2015.
[22] S. Mirjalili, "The ant lion optimizer," *Adv. Eng. Softw.*, vol. 83, pp. 80–98, May 2015.
[23] S. Mirjalili, S. M. Mirjalili, and A. Lewis, "Grey wolf optimizer," *Adv. Eng. Softw.*, vol. 69, pp. 46–61, Mar. 2014.
[24] S.-C. Chu, P.-W. Tsai, and J.-S. Pan, "Cat swarm optimization," in *Trends in Artificial Intelligence* (Lecture Notes in Computer Science), vol. 4099. Berlin, Germany: Springer, 2006, pp. 854–858.
[25] M. Dorigo and G. Di Caro, "Ant colony optimization: A new meta-heuristic," in *Proc. IEEE Congr. Evol. Comput.*, Washington, DC, USA, Jul. 1999, pp. 6–9.
[26] A. R. Mehrabian and C. Lucas, "A novel numerical optimization algorithm inspired from weed colonization," *Ecol. Inform.*, vol. 1, no. 4, pp. 355–366, Dec. 2006.
[27] P. J. van Laarhoven and E. H. Aarts, "Simulated annealing," in *Simulated Annealing: Theory Applications*. Dordrecht, The Netherlands: Springer, 1987, pp. 7–15.
[28] S. Mirjalili and A. Lewis, "The whale optimization algorithm," *Adv. Eng. Softw.*, vol. 95, pp. 51–67, May 2016.
[29] X.-S. Yang, "Bat algorithms," in *Nature-Inspired Optimization Algorithms*, 1st ed. Amsterdam, The Netherlands: Elsevier, 2014, pp. 141–154.
[30] T. van Luyen and T. V. B. Giang, "Null-Steering Beamformer Using Bat Algorithm," *Appl. Comput. Electromagn. Soc. J.*, vol. 33, no. 1, pp. 23–29, 2018.
[31] L. van Tong and V. B. G. Truong, "BAT algorithm based beamformer for interference suppression by controlling the complex weight," *REV J. Electron. Commun.*, vol. 7, no. 4, pp. 87–93, 2018.
[32] O. Alluhaibi, Q. Z. Ahmed, J. Wang, and H. Zhu, "Hybrid digital-to-analog precoding design for mm-Wave systems," in *Proc. IEEE Int. Conf. Commun. (ICC)*, Paris, France, May 2017, pp. 1–6.
[33] S.-C. Huang, W.-H. Fang, H.-S. Chen, and Y.-T. Chen, "Hybrid genetic algorithm for joint precoding and transmit antenna selection in multiuser MIMO systems with limited feedback," in *Proc. VTC-Spring*, Taipei, Taiwan, May 2010, pp. 1–5.
[34] C. Hong, Z. Wei, J. Geng, and D. Yang, "Multiuser hybrid phase-only analog/digital beamforming with genetic algorithm," in *Proc. IEEE PIMRC*, Washington, DC, USA, Sep. 2014, pp. 517–521.
[35] Z. Zhuang, Z. Wei, N. Li, and L. Sang, "Discrete phase-only hybrid BF method in MIMO system based on genetic algorithm," in *Proc. IEEE ICCT*, Chengdu, China, Oct. 2017, pp. 650–654.
[36] Y. Chen, Y. Xia, Y. Xing, and L. Yang, "Low complexity hybrid precoding for mmWave massive MIMO systems," in *Proc. IEEE WOCC*, Newark, NJ, USA, Apr. 2017, pp. 1–5.
[37] Z. Wang, M. Li, Q. Liu, and A. L. Swindlehurst, "Hybrid precoder and combiner design with low-resolution phase shifters in mmWave MIMO systems," *IEEE J. Sel. Topics Signal Process.*, vol. 12, no. 2, pp. 256–269, May 2018.
[38] X. Yu, J.-C. Shen, J. Zhang, and K. B. Letaief, "Alternating minimization algorithms for hybrid precoding in millimeter wave MIMO systems," *IEEE J. Sel. Topics Signal Process.*, vol. 10, no. 3, pp. 485–500, Apr. 2016.
[39] F. Shu, Z. Wang, R. Chen, Y. Wu, and J. Wang, "Two high-performance schemes of transmit antenna selection for secure spatial modulation," *IEEE Trans. Veh. Technol.*, vol. 67, no. 9, pp. 8969–8973, Sep. 2018.
[40] F. Shu, M. M. Wang, Y. X. Wang, H. Q. Fan, and J. H. Lu, "An efficient power allocation scheme for leakage-based precoding in multi-cell multiuser MIMO downlink," *IEEE Commun. Lett.*, vol. 15, no. 10, pp. 1053–1055, Oct. 2011.
[41] F. Shu, L. Xu, J. Wang, W. Zhu, and Z. Xiaobo, "Artificial-noise-aided secure multicast precoding for directional modulation systems," *IEEE Trans. Veh. Technol.*, vol. 67, no. 7, pp. 6658–6662, Jul. 2018.
[42] M. Alarfaj and H. Liu, "Subarray hybrid precoding for massive MIMO capacity maximization," in *Proc. IEEE 17th Int. Conf. Ubiquitous Wireless Broadband (ICUWB)*, Sep. 2017, pp. 1–5.
[43] K. Roth, H. Pirzadeh, A. L. Swindlehurst, and J. A. Nossek, "A comparison of hybrid beamforming and digital beamforming with low-resolution ADCs for multiple users and imperfect CSI," *IEEE J. Sel. Topics Signal Process.*, vol. 12, no. 3, pp. 484–498, Jun. 2018.
[44] K. Duan, H. Du, and Z. Wu, "Hybrid alternating precoding and combining design for mmWave multi-user MIMO systems," in *Proc. IEEE/CIC Int. Conf. Commun. China (ICCC)*, Aug. 2018, pp. 217–221.
[45] C. Gan, W. Cao, M. Wu, and X. Chen, "A new bat algorithm based on iterative local search and stochastic inertia weight," *Expert Syst. Appl.*, vol. 104, pp. 202–212, Aug. 2018.
[46] X.-B. Meng, X. Gao, Y. Liu, and H. Zhang, "A novel bat algorithm with habitat selection and Doppler effect in echoes for optimization," *Expert Syst. Appl.*, vol. 42, nos. 17–18, pp. 6350–6364, 2015.
[47] N. S. Grewal, M. Rattan, and M. S. Patterh, "A linear antenna array failure correction using improved bat algorithm," *Int. J. RF Microw. Comput.-Aided Eng.*, vol. 27, no. 7, 2017, Art. no. e21119.
[48] Y. Feng, G. Liao, J. Xu, S. Zhu, and C. Zeng, "Robust adaptive beamforming against large steering vector mismatch using multiple uncertainty sets," *Signal Process.*, vol. 15, pp. 320–330, Nov. 2018.
[49] M. Zhang, A. Zhang, and Q. Yang, "Robust adaptive beamforming based on conjugate gradient algorithms," *IEEE Trans. Signal Process.*, vol. 64, no. 22, pp. 6046–6057, Nov. 2016.
[50] B. D. Carlson, "Covariance matrix estimation errors and diagonal loading in adaptive arrays," *IEEE Trans. Aerosp. Electron. Syst.*, vol. AES-24, no. 4, pp. 397–401, Jul. 1988.
[51] X.-S. Yang and A. H. Gandomi, "Bat algorithm: A novel approach for global engineering optimization," *Eng. Comput.*, vol. 29, no. 5, pp. 464–483, 2012.
[52] J. Capon, "High-resolution frequency-wavenumber spectrum analysis," *Proc. IEEE*, vol. 57, no. 8, pp. 1408–1418, Aug. 1969.

MOHAMMED A. ALMAGBOUL received the B.Sc. degree (Hons.) in electronic engineering and the M.S. degree in communication engineering from the Sudan University of Science and Technology, Sudan, in 2005 and 2010, respectively. He is currently pursuing the Ph.D. degree with the Information and Communications Systems Department, Nanjing University of Science and Technology, Nanjing, China. Since 2007, he has been a Lecturer with the Electronic Engineering Department, Sudan Technological University, and a Lecturer with the Communication Engineering Department, AlMughtaribeen University, since 2014. His research interests include wireless communications networks, the Internet of Things, and signal processing.

FENG SHU was born in 1973. He received the B.S. degree from the Fuyang Teaching College, Fuyang, China, in 1994, the M.S. degree from Xidian University, Xi'an, China, in 1997, and the Ph.D. degree from Southeast University, Nanjing, China, in 2002. In 2005, he joined the School of Electronic and Optical Engineering, Nanjing University of Science and Technology, Nanjing, where he is currently a Professor, and also a Supervisor of the Ph.D. and graduate students. From 2009 to 2010, he held a visiting postdoctoral position with The University of Texas at Dallas. He has published about 300 articles, of which over 200 are in archival journals, including more than 60 articles in the IEEE journals and more than 100 SCI-indexed articles. He holds seven Chinese patents. His research interests include wireless networks, wireless location, and array signal processing. He serves as a TPC Member for several international conferences, including the IEEE ICC 2019, the IEEE ICCS 2018/2016, ISAPE 2018, and WCSP 2017/2016/2014. He was a Mingjiang Chair Professor in Fujian Province. He is currently an Editor of the journal IEEE Access.

YAOLU QIN received the B.S. degree from Nanjing Normal University, Nanjing, China, in 2016. She is currently pursuing the M.S. degree with the School of Electronic and Optical Engineering, Nanjing University of Science and Technology, China. She is also with the School of Electronic and Optical Engineering, Nanjing University of Science and Technology. Her research interests include wireless localization, wireless communication, and mobile networks.

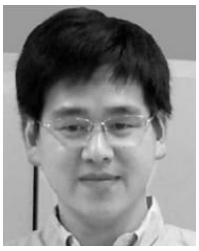

XIAOBO ZHOU received the M.S. degree from the School of Electronic Science and Engineering, Anhui University, China, in 2010. He is currently pursuing the Ph.D. degree with the School of Electronic and Optical Engineering, Nanjing University of Science and Technology. Since 2010, he has been a Teacher with the School of Physics and Electronic Engineering, Fuyang Normal University. His main research interests include physical layer security and energy harvesting.

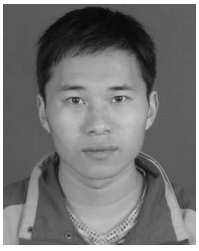

JIN WANG received the B.S. and Ph.D. degrees from the School of Electronic and Optical Engineering, Nanjing University of Science and Technology, Nanjing, China, in 2012 and 2019, respectively. He is currently with the Shanghai Aerospace Electronic Technology Institute, Shanghai, China. His research interests include wireless communications and signal processing.

YUWEN QIAN received the Ph.D. degree in automatic engineering from the Nanjing University of Science and Technology, Nanjing, China, in 2011, where he was a Lecturer, from July 2002 to June 2011. Since October 2011, he has been a Lecturer with the School of Electronic and Optical Engineering, Nanjing University of Science and Technology. His main research interests include information security, smart grids, and power line communications.

KINGSLEY JUN ZOU received the Ph.D. degree from the Wireless Networking and Mobile Communications Group, School of Electronic and Optical Engineering, Nanjing University of Science and Technology. Since 2016, he has been with the Wireless Networking and Mobile Communications Group, Nanjing University of Science and Technology, where he is currently a Lecturer with the School of Electronic and Optical Engineering. He has over ten IEEE journal publications. His research interests include wireless communications, signal processing, and the Internet of Things.

ABDELDIME MOHAMED SALIH ABDELGADER received the B.S. degree in electronic engineering from the Sudan University of Science and Technology, Khartoum, Sudan, in 2000, the M.S. degree in communication engineering from Karary University, Omdurman, Sudan, in 2003, and the Ph.D. degree from the School of Information Science and Communication Engineering, Southeast University, Nanjing, China, in 2016. Since 2003, he has been a Lecturer with the Department of Electrical and Computer Engineering, Karary University. He is a Visiting Postdoctoral Fellow with the Nanjing University of Science and Technology. His research interests include wireless communication networks, network security, and the physical layer of the vehicular networks. Besides the academic degrees, he has many other certificates, such as CCNA, CCNA Sec., CCNP, the Sudanese Engineering Society Award, and others.